

# Eu<sup>3+</sup> Luminescence Measurements In La<sup>3+</sup>/Eu<sup>3+</sup> - Y Zeolites

Oswaldo A. Serra\* , Ieda L.V. Rosa

*Departamento de Química da FFCLRP de Universidade de São Paulo,  
Av. Bandeirantes 3900, 14040-901 Ribeirão Preto, SP Brasil*

and

Eduardo F. Sousa-Aguiar

*DICAT-CENPES Petrobras S.A., Ilha do Fundão Q7, Rio de Janeiro, RJ, Brasil*

Received: october 18, 1993

Zeólitas Y ionicamente trocadas com terras raras, RE-Y, foram estudadas através da luminescência. Eu<sup>3+</sup> foi usado como sonda a fim de obter informações a respeito da posição dos íons lantanídicos. As análises das várias transições características do Eu<sup>3+</sup> revelaram que tratamentos térmicos diferentes levam a diferentes sítios RE nas zeólitas. A presença de vapor no processo de calcinação, após a troca com a terra rara, aparentemente promoveu a migração dos íons RE para sítios mais internos. As zeólitas calcinadas a seco mostraram uma maior dependência com relação à temperatura. As medidas de tempo de vida revelaram que a calcinação a vapor também conduz a uma maior homogeneidade de sítios.

Rare Earth - exchanged Y zeolites, RE-Y, have been studied by means of luminescence spectroscopy. Eu<sup>3+</sup> was used as a probe ion in order to obtain information concerning to the position of lanthanum ions. The analysis of several characteristic Eu<sup>3+</sup> transitions revealed that distinct thermal treatments cause different RE sites. The presence of steam in the dehydration step after the RE exchanged apparently promoted the migration of RE ions to more internal sites. Dry dehydrated zeolites show a stronger dependence on temperature. Lifetime measurements revealed that the steam dehydration also led to more homogeneous sites.

**Key words:** *Y zeolite; luminescence; europium III.*

## Introduction

Nowadays, zeolites play a fundamental role in many industries such as detergent<sup>1</sup>, paper<sup>2</sup> and especially petrochemical<sup>3,4</sup>. Fluid Cracking Catalysts (FCC) have as main component the Y type synthetic zeolites. These industrial compounds are in the Na<sup>+</sup> form, NaY, which is catalytically inactive in many reactions. The conversion to an active form is carried out by exchange with polyvalent cations, such as trivalent rare earth ions<sup>5</sup>. The hydrolysis of these hydrated ions through dehydration leads to the formation of Bronsted and/or Lewis acid sites<sup>6</sup> which are then responsible for the catalytic properties.

The hydrated rare earth ions are initially in the supercages or cages, that have an internal diameter of 12.5 Å. After heating, these ions lose water and go to the more internal cages, known as sodalite or cages with a diameter of 6.5 Å. It is also possible, but less probable, that they are accommo-

dated in the hexagonal prisms, diameter of 2.5 Å. The formation of bonds between rare earth ions and lattice oxygen increases the zeolite structural stability<sup>7</sup>.

The luminescent properties of Eu<sup>3+</sup> and Tb<sup>3+</sup> are being used as structural probes in many systems<sup>8,9</sup>. Eu<sup>3+</sup> is the most studied by luminescence spectroscopy among the rare earth ions, owing to the simplicity of its spectra and because of its application as red phosphor in TV screens<sup>10</sup>.

The emission spectra of the Eu<sup>3+</sup> are a very sensitive indicator of its environment. Normally, in inorganic systems, the ion excited by 394nm light (<sup>5</sup>L<sub>6</sub> level) decays to the <sup>5</sup>D levels, mainly to the <sup>5</sup>D<sub>0</sub>, from which the ground state is reached with emission of radiation to the levels of the fundamental<sup>11</sup> term <sup>7</sup>F<sub>J</sub> (J=0-6). The (2J+1) degenerescence of the free ion may be broken by the crystal field at its location. The levels with J=0 are not degenerated, and the <sup>5</sup>D<sub>0</sub> → <sup>7</sup>F<sub>0</sub> transition shows no more than one band, <sup>5</sup>D<sub>0</sub> → <sup>7</sup>F<sub>1</sub> three bands and <sup>5</sup>D<sub>0</sub> → <sup>7</sup>F<sub>2</sub> five bands, providing that the Eu<sup>3+</sup>

sites have a unique symmetry and that there are no vibrational bands<sup>12</sup>. The ratio between the intensities of  ${}^5D_0 \rightarrow {}^7F_1/{}^7F_2$  emission is very sensitive to the environment of the  $\text{Eu}^{3+}$  because of the hypersensitive character of the  $0 \rightarrow 2$  transition<sup>13</sup>. The  $0 \rightarrow 1$  transition preserves its magnetic dipole character and its intensity is almost independent of the environment. The  $0 \rightarrow 2$  is always of electric dipole character. The  $0 \rightarrow 0$  is allowed only in low symmetry and its intensity is also very dependent on the environment<sup>14</sup>.

Zeolites and other silica/alumina catalysts have been studied by  $\text{Eu}^{3+}$  luminescence<sup>15,16</sup>. An important review<sup>17</sup> deals with the use of luminescence to obtain information on the structure of zeolites. Arakawa et al.<sup>18-21</sup> studied the interaction of  $\text{Eu}^{3+}$  and zeolitic water in vacuum at 300 °C. Suib et al.<sup>22</sup> combining lifetime and EXAFS data, determined the  $\text{Eu}^{3+}$  coordination in A and Y zeolites. Bartlett et al.<sup>13</sup>, observing the  $0 \rightarrow 0$  transition, concluded that the  $\text{Eu}^{3+}$  is in the I' sites only and in both I' and II sites respectively in Y and X zeolites. The interaction of dehydrated Y zeolites with oxygen led Ozin<sup>23</sup> to consider the  $\text{Eu}^{3+}$  in sites I, I' and II with low symmetries such as  $C_{nv}$ ,  $C_n$  or  $C_s$  and also that the  $\text{Eu}^{3+}$  migrates from the beta to the alpha cages with oxygenation.

Luminescence lifetime measurements of RE in biological systems can give information about the water molecules around the RE ion<sup>8,9</sup>. This technic was applied here to determine the  $\text{Eu}^{3+}$  hydration number in the  $\text{La}^{3+}/\text{Eu}^{3+}$ -Y zeolites.

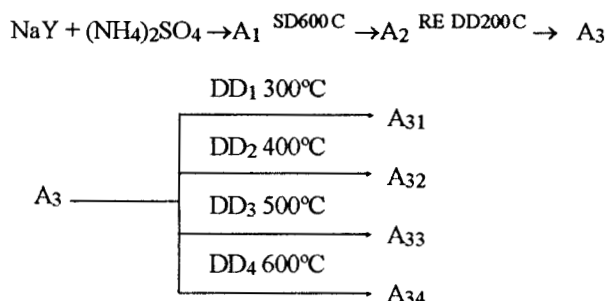
In this paper, we describe the use of  $\text{Eu}^{3+}$  luminescence in  $\text{La}^{3+}/\text{Eu}^{3+}$ -Y zeolites in order to obtain useful information about the RE behavior related to various physicochemical treatments for zeolite activation.

## Experimental

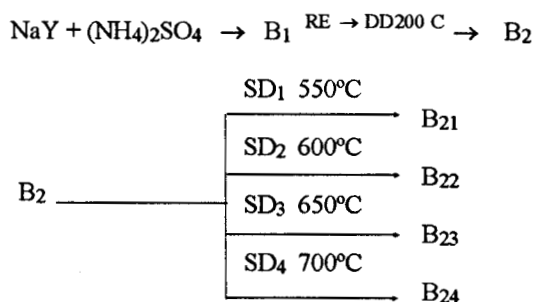
**RE-Y exchanged zeolites:** Na-Y zeolite (Silica/Alumina, SAR=5,0) was exchanged three times with  $(\text{NH}_4)_2\text{SO}_4$  in pH 4,5 and followed by another exchange with  $\text{Eu}_1\text{La}_9\text{Cl}_3$  in pH 5,0. The exchange with the rare earth (RE) was performed before or after the thermal treatment of the zeolite, in the presence or absence of steam. Schemes 1 and 2 show how the zeolites were submitted to the physicochemical treatments.

**Luminescence Spectra:** A SPEX FLUOROLOG II was used to measure the emission spectra (550-750 nm) for excitation by 394 nm light. For the excitation spectra the emission wavelength was 612 nm. The spectra were taken at

### Scheme 1. Dry Dehydration - DD:



### Scheme 2. Steam Dehydration - SD:



25 °C and under liquid nitrogen temperature from samples in 1mm quartz tubes.

**Luminescence Lifetime Measurements:** Experiments were performed at liquid nitrogen using a Spex fluorolog II connected with an 1934D Phosphorimeter. The excitation and emission wavelengths were 394 and 612 nm, respectively.

**Y zeolite characteristics:** All of the zeolites samples had  $(90 \pm 10)\%$  of crystallinity, unit cell size,  $A_0 = (24,6 \pm 0.1)$  Å, and RE contents of 2.7 wt % (series A) and 3.3 wt % (series B).

## Results and Discussion

Figure 1 shows the excitation spectrum of  $\text{Eu}^{3+}$  in the A<sub>34</sub> zeolite at liquid nitrogen. The excitation spectra of all samples are very similar. The maximum excitation was observed at 394 nm, corresponding to the level  ${}^5L_6$ , as expected for inorganic compounds. The emission spectra of  $\text{Eu}^{3+}$  in the samples A<sub>3</sub>, A<sub>31</sub>, A<sub>32</sub> and A<sub>33</sub> at liquid nitrogen are represented by A<sub>34</sub> spectrum, which is shown in Figure 2. The spectrum of the B<sub>24</sub> sample is shown in Figure 3, representing the B series. Since the intensity of the  $0 \rightarrow 1$  magnetic dipole transition is almost independent of the environment, the intensities of the other transitions are normalized to it<sup>24,25</sup>. The bandwidths were very large, as expected for these materials, in contrast to the ion in well-defined crystals<sup>26-28</sup>. The relative areas (RA) and the bandwidths (BW) for the 0, 1, 2 transitions are presented in Table 1.

In Figures 2 and 3 one observes that the bandwidth of the

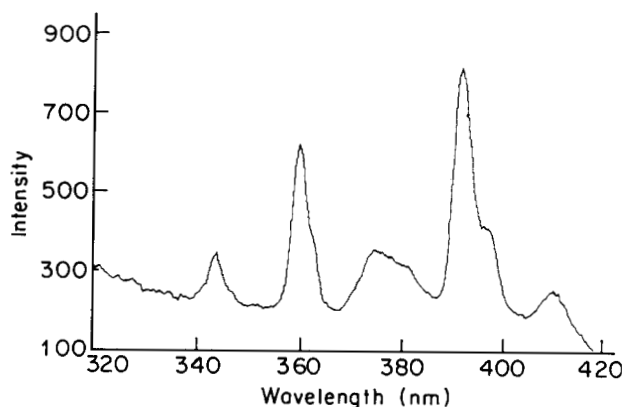


**Figure 1.** Excitation spectrum of the  $\text{Eu}^{3+}$  in A<sub>34</sub> zeolite,  $\lambda_{em} = 612$  nm, at liquid nitrogen..

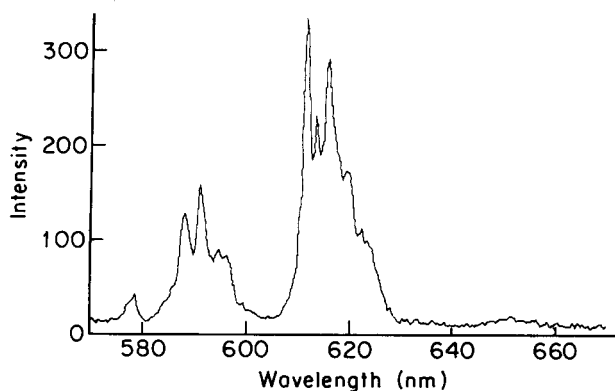
**Table 1.** Relative areas (RA) and bandwidths (BW),  $\text{cm}^{-1}$ , for the  $\text{Eu}^{3+} \ ^5D_0 \rightarrow \ ^7F_{0,1,2}$  emissions in the series A (DD) and B (SD)  $\text{Eu}_x\text{La}_{1-x}\text{Y}$  zeolites.

	A <sub>3</sub>		A <sub>31</sub>		A <sub>32</sub>		A <sub>33</sub>		A <sub>34</sub>	
	RA	BW	RA	BW	RA	BW	RA	BW	RA	BW
J = 0	0.05	120	0.05	120	0.10	162	0.11	270	0.16	223
J = 1	1.00	579	1.00	612	1.00	702	1.00	648	1.00	676
J = 2	2.84	913	5.47	925	4.92	903	4.99	954	5.49	986

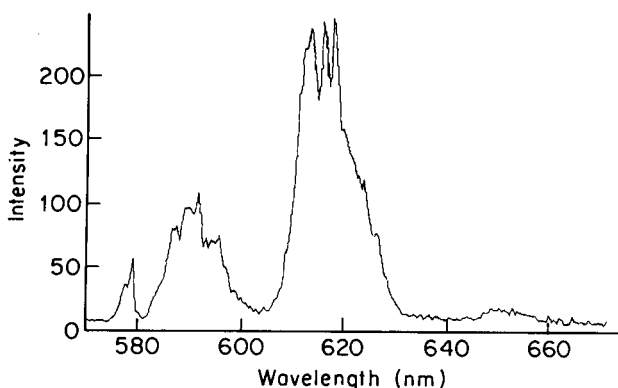
  

	B <sub>2</sub>		B <sub>21</sub>		B <sub>22</sub>		B <sub>23</sub>		B <sub>24</sub>	
	RA	BW	RA	BW	RA	BW	RA	BW	RA	BW
J = 0	0.05	78	0.10	241	0.11	216	0.12	210	0.13	198
J = 1	1.00	535	1.00	600	1.00	657	1.00	657	1.00	618
J = 2	2.74	986	4.02	986	4.35	991	4.73	995	4.62	972

$0 \rightarrow 0$  transition is wider in A<sub>3</sub> than in B<sub>2</sub> (Table 1), in agreement with a larger number of sites in A<sub>3</sub>. The zeolite A<sub>3</sub> is heated in the presence of steam before the exchange with the RE (Scheme 1). This treatment gives rise to deformations in the zeolite structure, creating mesoporosities and a slight contraction in the unit cell, leading to a more different



**Figure 2.** Emission spectrum of the  $\text{Eu}^{3+}$  in A<sub>34</sub> zeolite,  $\lambda_{\text{ex}} = 394 \text{ nm}$ , at liquid nitrogen.



**Figure 3.** Emission spectrum of the  $\text{Eu}^{3+}$  in B<sub>24</sub> zeolite,  $\lambda_{\text{ex}} = 394 \text{ nm}$ , at liquid nitrogen.

range of sites or to a greater number of distinct sites in A<sub>3</sub> than in B<sub>2</sub> (Scheme 2). A broadening of all bands with the increase of dehydration temperature for series A and B (Table 1) indicates an increasing number of distinct sites. We considered that the presence of water and hydroxyl groups are probably responsible for the large difference in the bandwidth ( $0 \rightarrow 0$ ) for the samples A<sub>3</sub> ( $120 \text{ cm}^{-1}$ ) and A<sub>34</sub> ( $223 \text{ cm}^{-1}$ ). In the series B the bandwidth differences are owing to the dealumination of the structure by heating at  $700^\circ\text{C}$  in the presence of steam.

Figure 4 presents the RA of the  $0 \rightarrow 0$  transition as a function of dehydration temperature for the series A<sub>3</sub> and B<sub>2</sub>. The greater slope of A<sub>3</sub> relative to B<sub>2</sub> shows that the occupation of the sites of the dry dehydrated samples is strongly dependent on the temperature.

The growth of the RA of the  $0 \rightarrow 0$  with the increasing dehydration temperature, is related to a lowering of symmetry at the  $\text{Eu}^{3+}$  and/or an augmenting in the number of occupied distinct sites. The water molecules and the hydroxyl

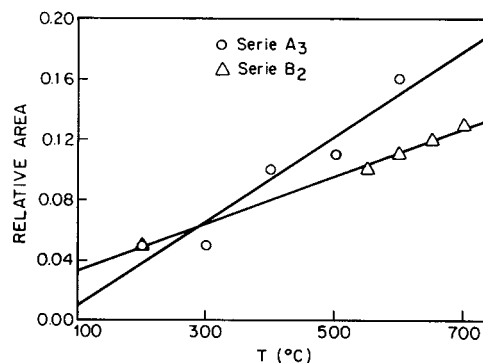


**Figure 4.** Area of the  $^5D_0 \rightarrow ^7F_0$  transition relative to  $^5D_0 \rightarrow ^7F_1$ , as a function of the dehydration temperature, for the A<sub>3</sub> (DD) (○) and B<sub>2</sub> (SD) (△) zeolites.

groups behave as quenchers for the  $\text{Eu}^{3+}$  emission. With the reduction of water, some  $\text{Eu}^{3+}$  migrates to more internal positions, binding to structural oxygen, consequently having less non-radiative loss by vibrational mechanisms.

The emission spectra of  $\text{Eu}^{3+}$  (Figs. 2 and 3) contain more information about the site symmetry. If one observes more than one band and/or a broadening of the  $0 \rightarrow 0$  transition, it is certainly due to the presence of sites with more than one symmetry. For all studied zeolites, this band was broad and asymmetric (even at liquid nitrogen), indicating the presence of several sites of low symmetry such as  $C_s$ ,  $C_{nv}$  and/or  $C_n$ , in agreement with Ozin et al.<sup>22</sup>

Figure 5 shows the luminescence decay with time for the  $^5D_0 \rightarrow ^7F_2$   $\text{Eu}^{3+}$  transition ( $\lambda_{\text{ex}} = 394 \text{ nm}$ ,  $\lambda_{\text{em}} = 612 \text{ nm}$ ) in A<sub>34</sub> (a) and B<sub>24</sub> (b) samples. A<sub>34</sub> zeolite presents a decay with a double exponential function, whose lifetimes are 0.74 and 2.51 ms, respectively for the first and second exponential. These results indicate the presence of at least two different  $\text{Eu}^{3+}$  sites in the A<sub>34</sub> (DD) sample. In one of them the  $\text{Eu}^{3+}$  is coordinated to one water molecule ( $t = 0,74 \text{ ms}$ )<sup>8</sup>; in the other the  $\text{Eu}^{3+}$  ion is in the absence of coordinated water ( $t = 2,51 \text{ ms}$ ). The sample B<sub>24</sub> (SD) presents a single exponen-

tial function whose lifetime is 0.74 ms, indicating the presence of one water molecule at the  $\text{Eu}^{3+}$  environment.

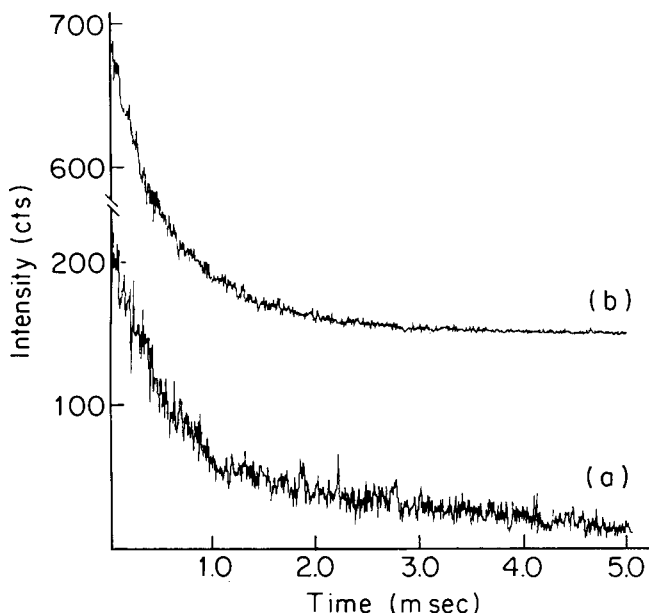


**Figure 5.** Luminescence decay curve for the  $\text{Eu}^{3+} \ ^5D_0 \rightarrow \ ^7F_2$  transition,  $\lambda_{\text{ex.}} = 394 \text{ nm}$ ,  $\lambda_{\text{em.}} = 612 \text{ nm}$ , in  $A_{34}$  (a) and  $B_{24}$  (b) samples

### Conclusion

The different thermal treatments of the zeolites containing RE lead to symmetry differences in the sites where the rare earth is positioned. In the  $B_2$  series, steam dehydrated, the RE ions remain bounded to the water molecules even at under higher temperatures; moving to more internal sites where they are fixed to the structural oxygens. In the  $A_3$  series, dry dehydrated, the ions lose the water molecules more easily, also undergoing the formation of hydroxyl groups. These groups inhibit the ion movement to small cavities. With the increase of the temperature, the ion will be fixed on or near the supercages. The steam dehydrated samples,  $B_2$ , presents a more homogeneous type of site. In all of our assumptions the sizes of the hydrated  $\text{Eu}^{3+}$  and  $\text{La}^{3+}$  were considered similar. This allows the use of  $\text{Eu}^{3+}$  as a structural probe, since the size of the zeolite and cages are also larger than the hydrated ions.

### Acknowledgments

We are grateful to CAPES, CNPq and PETROBRAS for financial support and fellowship grants (ILVR).

### References

1. I. A. Maxwell, *Adv. Catal.* **31**, 1 (1982).
2. P. Gallezot, *Catal. Rev. - Sci. Eng.* **20**, 121 (1979).
3. M. J. Scherger, H. G. Smolka. *The Properties and Applications of Zeolites* (R.P. Townsed, London, 1980).
4. Z. Quanchang, S. Minqdi, D. Changlu, Y. Huari, Z. Qixing Z. Zhiguo, in S. Hocevar and S. Pejovnik, (eds).

*Zeolites: Synthesis, Structure, Technology and Application* (Elsevier, Amsterdam, 1985).

5. H. W. Haynes Jr., *Catal. Rev. - Sci. Eng.* **17**, 273 (1978).
6. J. W. Ward, *J. Catal.* **13**, 321 (1969).
7. C. V. McDaniel, P. K. Maher, *Zeolite Chemistry and Catalysis*. ACS Monograph. **171** (Washington DC, 1976).
8. W. de W. Horrocks Jr., D. R. Sudnick, *Acc. Chem. Res.* **14**, 384 (1981).
9. W. de W. Horrocks Jr., M. Albin, *Prog. Inorg. Chem.* **31**, 1 (1984).
10. G. Blasse, A. Bril, *Philips Tech. Rev.* **31**, 304 (1970).
11. A. Bril, W. L. Wanmaker, *Philips Tech. Rev.* **27**, 22 (1966).
12. F. S. Richardson, *Chem. Rev.* **82**, 541 (1982).
13. J. R. Bartlett, R. P. Cooney, R. A. Kidd, *J. Catal.* **114**, 58 (1988).
14. F. S. Richardson, H. G. Brittain, *J. Am. Chem. Soc.* **103**, 18 (1981).
15. F. Bergaya, H. Van Demme, *J. Chem. Soc., Faraday Transl. II*, **79**, 505 (1983).
16. G. T. Pott, W. H. Stork, *Catal. Rev. - Sci. Eng.* **12**, 163 (1975).
17. J. F. Tanguay, S. L. Suib, *Catal. Rev. - Sci. Eng.* **29**, 1 (1987).
18. T. Arakawa, M. Takakuwa, G.-Y. Adachi, J. Shiokawa, *Bull. Chem. Soc. Japan* **57**, 1290 (1984).
19. T. Arakawa, T. Takata, M. Takakuwa, G.-Y. Adachi, J. Shiokawa, *Mater. Res. Bull.* **17**, 171 (1982).
20. T. Arakawa, T. Takata, G.-Y. Adachi, J. Shiokawa, *J. Luminescence.* **20**, 325 (1979).
21. T. Arakawa, T. Takata, G.-Y. Adachi, J. Shiokawa, *J. Chem. Soc., Chem. Commun.* **453** (1979).
22. S. L. Suib, R. P. Zerger, G. D. Stucky, T. I. Morrison, G. K. Shenoy, *J. Chem. Phys.* **80**, 2203 (1984).
23. G. A. Ozin, M. D. Baker, M. M. Olken, *J. Am. Chem. Soc.* **110**, 5709 (1988).
24. R. Reisfeld, *Struct. Bonding* **30**, 65 (1979).
25. G. Blasse, *Solid State Chem.* **3**, 153 (1982).
26. O. A. Serra, L. C. Thompson, *Inorg. Chem.* **15**, 504 (1976).
27. Y. Haas and G. Stein, *J. Phys. Chem.* **75**, 3677 (1971).
28. G. Stein and E. Wurzburg, *J. Chem. Phys.* **62**, 208 (1975).